JOURNAL OF MATERIALS SCIENCE **35** (2000) 685–692

Sulphidation and oxidation of the Ni22Cr10Al1Y alloy in H_2/H_2S and SO_2 atmospheres at high temperatures

Z. ŻUREK
Cracow University of Technology, ul. Warszawska 24, 31-155 Kraków, Poland

J. JEDLIŃSKI*, K. KOWALSKI
Surface Spectroscopy Lab, Jagellonian University, ul. Reymonta 23, 30-059 Kraków, Poland; University of Mining and Metallurgy, Kraków, Poland
E-mail: jedlinsk@uci.agh.edu.pl

V. KOLARIK, W. ENGEL
Fraunhofer-Institut für Chemische Technologie, Pfinztal, Germany

J. MUSIL
Škoda, Research, Plzen Ltd. Plzen, Czech Republic

The Ni22Cr10Al1Y alloy was exposed in H_2/H_2S gas mixture under the sulphur pressure 10^{-3} and 1 Pa as well as in SO_2 at 1173 and 1273 K. At $p_{s_2} = 1$ Pa the sulphidation rate was relatively high and the reaction obeyed the linear rate law. Under these conditions a nickel/nickel sulphide eutectic was formed. At $p_{s_2} = 10^{-3}$ Pa nickel sulphides became unstable and the sulphidation rate was significantly lower. The reaction obeyed the parabolic rate law. The oxidation rate of the alloy in SO_2 was lower than that in any of the H_2/H_2S atmospheres. The sulphide scales formed during sulphidation in H_2/H_2S had complex microstructures and compositions, with sulphospinel and sulphide phases being present, e.g. $NiCr_2S_4$, Ni_3S_2, Cr_xS_y. As the temperature increased and the sulphur pressure decreased, these phases were replaced by the chromium-rich sulphide phase. Various oxides formed during oxidation of the alloy in SO_2.

1. Introduction

Despite of the many intensive studies on the corrosion resistance of different metallic materials, the way to find the alloys satisfying fully the demands of modern technologies seems still far away.

The efficient use of materials is traditionally associated with an effective process of material selection. The selection criterion for bond coat materials in thermal barrier coating systems is their ability to withstand corrosion by hot aggressive atmospheres. In particular, oxidation-sulphidation attack can be a major problem. Compositional flexibility of the MCrAl(X) bond coatings (with M = Ni, Co and X = Y, Hf etc.) makes them suitable for a great variety of service conditions.

The presence of aluminium in these alloys provides good oxidation resistance which can be still further improved by small additions of the, so-called, reactive elements (Y, Hf, Ce etc.). Relatively high content of chromium provides some resistance against hot-corrosion. The proper Cr/Al ratio allows for flexible control of the alloy composition which gives an opportunity to improve the anticorrosive properties required for different environments at high temperatures. The process of oxidation of such alloys (bulk materials or thin layers) has been the subject of numerous studies in different research centres, e. g. [1–4]. However, the corrosion of these alloys in the atmospheres containing sulphur was studied to a significantly lesser extent.

In this paper, the results of the study of Ni22Cr10AlY alloy corrosion in the atmosphere of "pure" SO_2 and in H_2/H_2S mixtures at different sulphur partial pressures are presented. The meaning of term "pure" should be understood as described below.

As far as the exposure in SO_2 is concerned, it is usually assumed in the literature [5], that the partial pressures of oxygen and sulphur are determined by the following dissociation equilibrium:

$$2SO_2 \Leftrightarrow S_2 + 2O_2$$

It should, however, be noted that even if pure SO_2 is heated to high temperatures, partial pressures of O_2 and S_2 are not only due to the dissociation of SO_2.

It has been pointed out [5–7] that in SO_2 some secondary reactions take place leading to the formation of multicomponent gas mixture, in which the ratio of

* Author to whom all correspondence should be addressed.

oxygen to sulphur partial pressures differs considerably from that derived from the dissociation of SO_2 only. In pure SO_2 or in $SO_2 + O_2$ gas mixture the following reactions take place simultaneously:

$$2SO_2 \Leftrightarrow S_2 + 2O_2$$
$$2SO_2 + O_2 \Leftrightarrow 2SO_3$$
$$2S_2 + O_2 \Leftrightarrow 2S_2O$$
$$S_2 + O_2 \Leftrightarrow 2SO$$

As a result, the following compounds can be present in the gaseus atmosphere: SO_2, O_2, SO_3, SO and S_2O. When partial pressure of oxygen is relatively high, some reaction can be neglected due to their small influence on the partial pressure of O_2 and S_2, whereas none of the reactions mentioned above can be ignored when dealing with pure or slightly oxygen-contaminated sulphur dioxide.

2. Experimental procedure

The alloys having the nominal composition Ni-22Cr-10Al-1Y (in wt.%) were deposited on a steel substrate by means of the Air Plasma Spraying (APS) method. The steel substrate was cleaned and slightly grit blasted before spraying. Powders PT 2872 (Ni22Cr 10Al1Y, powder size 45–104 μm) and AMDRY 962 (Ni22Cr10Al1Y, powder size 0–45 μm) were used for deposition. The coatings were peeled off when their thickness reached 1 mm. The morphology of the deposited materials (surface and polished cross-section) was examined using the Scanning Electron Microscope (SEM) and the distribution of alloy components was observed using the Energy Dispersive X-ray Spectrometry (EDX) methode. The materials consisted of layers in form of lamellas which result from the impact of the droplets on the substrate or on the prior solidified lamellas. The finer particle size of NiCrAlY powder provided a finer microstructure with high number of small pores and higher content of oxides which were formed during spraying process. The coarser powder provided a coarser microstructure with few large pores. Thus, two materials containing different porosity and grain size were obtained, one with higher porosity and coarser grains, and another exhibiting lower porosity and finer grains. The phase structure of both materials was studied by X-Ray Diffractometry (XRD) method. It was found that the materials were heterogeneous and contained the γ-Ni phase enriched in chromium with small amounts of β-NiAl. The material with finer particle size contained considerable amounts of elementary nickel.

The sulphidation process was carried out at temperatures 1173 K and 1273 K in H_2/H_2S atmospheres at two different sulphur vapour pressures: $p_{S_2} = 10^{-3}$ Pa (where the nickel sulphide is thermodynamically unstable) and $p_{S_2} = 1$ Pa (where the sulphides of all alloy components may be formed). The sulphidation exposures were performed in the apparatus described elsewhere [8]. Their duration depended on the reaction rate and varied from a period of few hours at high sulphur pressures to twenty hours at low sulphur pressures.

The oxidation studies of the materials in "pure" SO_2 were carried out for an exposure period of 30 h. The details of the experimental methods have been given in a previous paper [8].

3. Results

3.1. Kinetics

Representative kinetic data is shown in Figs 1 and 2 for exposures in H_2/H_2S gas mixtures and SO_2 atmosphere respectively.

The thermogravimetric studies in H_2/H_2S atmosphere for the both materials indicate that the process may be described generally by a parabolic law except for the material of lower porosity and smaller grains at $p_{S_2} = 1$ Pa and 1273 K (Fig. 1b). At the initial stage of the process, the observed deviations from this law may be due to the porosity of materials. At $p_{S_2} = 1$ Pa and 1273 K, material having lower porosity and smaller grains sulphidised according to the linear law; after 30 minutes the whole specimen was practically consumed which was not the case for the material of higher porosity and coarser grains, exposed under the same conditions. The latter was not completely consumed even after 120 minutes exposure. At

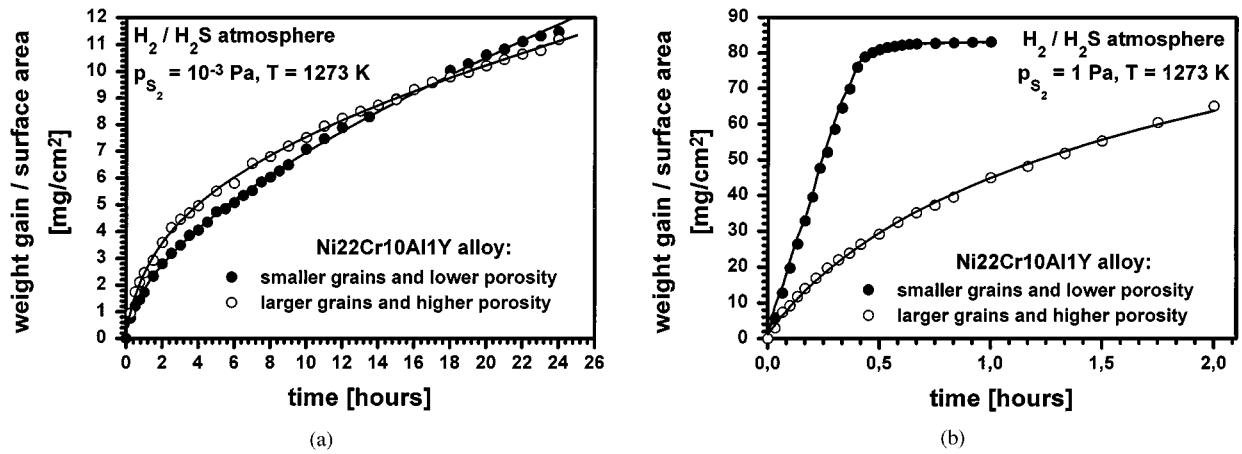

Figure 1 Sulphidation kinetics of the both Ni22Cr10Al1Y alloys in H_2/H_2S atmosphere at 1273 K: a) at $p_{S_2} = 10^{-3}$ Pa, b) at $p_{S_2} = 1$ Pa.

TABLE I Identification of oxide and sulphide phases formed on Ni22Cr10Al1Y alloy using X-ray diffraction method

Material	Exposure conditions	Detected phases	X-ray spectrum
Lower porosity and smaller grains	SO_2, 1173 K	NiO, Cr_2O_3, $NiCr_2O_4$ (t), $NiCr_2O_4$ (c)	From the surface
	SO_2, 1273 K	Al_2O_3, $NiCr_2O_4$ (t), Cr_2O_3	From the surface
	SO_2, 1273 K	Al_2O_3, Ni_3S_2 (r), $NiCrO_3$, NiO, Cr_2S_3 (r), $NiCr_2S_4$, $Y_3Al_5O_{12}$	From powdered scale
Higher porosity and larger grains	H_2/H_2S mixture $p_{S_2} = 1$ Pa, 1173 K	Ni_3S_2, Ni_3S_4	From the surface
	H_2/H_2S mixture $p_{S_2} = 1$ Pa, 1173 K	Ni_3S_2 (r), Al_2S_3 (t), Cr_2S_3 (r), $NiCr_2S_3$	From powdered scale
	H_2/H_2S mixture $p_{S_2} = 1$ Pa, 1273 K	Ni_3S_2, Ni_3S_4	From the surface
	H_2/H_2S mixture $p_{S_2} = 1$ Pa, 1273 K	Ni_3S_2 (r), Al_2S_3 (t), Cr_2S_3 (r), $NiCr_2S_4$	From powdered scale
	H_2/H_2S mixture $p_{S_2} = 10^{-3}$ Pa, 1173 K	CrS, Cr_7S_8, Cr_5S_6	From the surface
	H_2/H_2S mixture $p_{S_2} = 10^{-3}$ Pa, 1273 K	CrS, Cr_7S_8, Cr_5S_6, $NiCr_2S_4$	From the surface
	H_2/H_2S mixture $p_{S_2} = 10^{-3}$ Pa, 1273 K	Cr_7S_8	From powdered scale
Lower porosity and smaller grains	H_2/H_2S mixture $p_{S_2} = 10^{-3}$ Pa, 1173 K	Ni_3S_2 (r), $NiCr_2S_4$, Cr_7S_8	From the surface
	H_2/H_2S mixture $p_{S_2} = 1$ Pa, 1173 K	Ni_3S_2 (r), Al_2S_3 (t), Cr_2S_3 (r), $NiCr_2S_4$	From powdered scale
	H_2/H_2S mixture $p_{S_2} = 1$ Pa, 1273 K	Ni_3S_2 (r), Al_2S_3 (t), Cr_2S_3 (r), $NiCr_2S_4$	From powdered scale
	H_2/H_2S mixture $p_{S_2} = 10^{-3}$ Pa, 1273 K	Cr_7S_8	From powdered scale

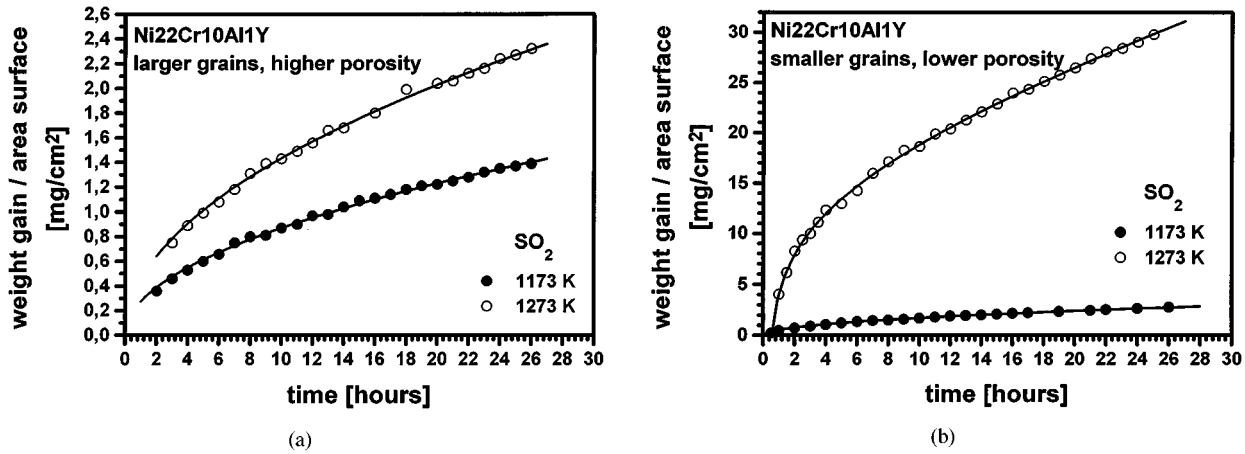

Figure 2 Oxidation kinetics of the Ni22Cr10Al1Y alloys in SO_2 at 1173 and 1273 K: a) material having larger grains and higher porosity, b) material having smaller grains and lower porosity.

$T = 1173$ K and $p_{S_2} = 1$ Pa, both materials sulphidised according to the parabolic law. For the sulphur partial pressure $p_{S_2} = 10^{-3}$ Pa the sulphidation process followed the parabolic rate law at both temperatures (Fig. 1a).

The oxidation of both materials in SO_2 followed the parabolic law at all temperatures (Fig. 2). Only during the initial reaction stages small deviations from this law were observed. As expected, the oxidation rate increased with the reaction temperature. The alloy having lower porosity and smaller grains oxidised apparently faster than the alloy exhibiting higher porosity and coarser grains.

3.2. Morphology and phase composition

The phase composition of scales formed on the studied materials was determined using the XRD method. The X-ray spectra were taken from the scale surfaces or/and powdered scales. The results are gathered in Table I.

The morphology, microstructure and composition of the scales were investigated by means of SEM and EDX techniques applied for surfaces and cross-sections of the samples. The scale morphology and microstructure were found to depend mainly on the sulphur vapour pressure in H_2/H_2S atmosphere and not on the reaction temperature. The SEM images and EDX analysis of the surface and corss-section, respectively, of the material

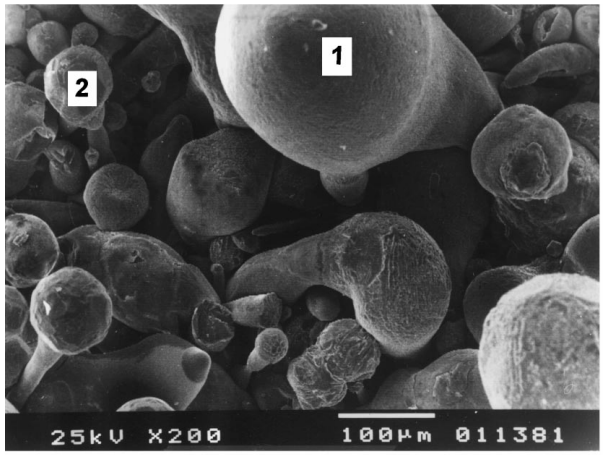

(a)

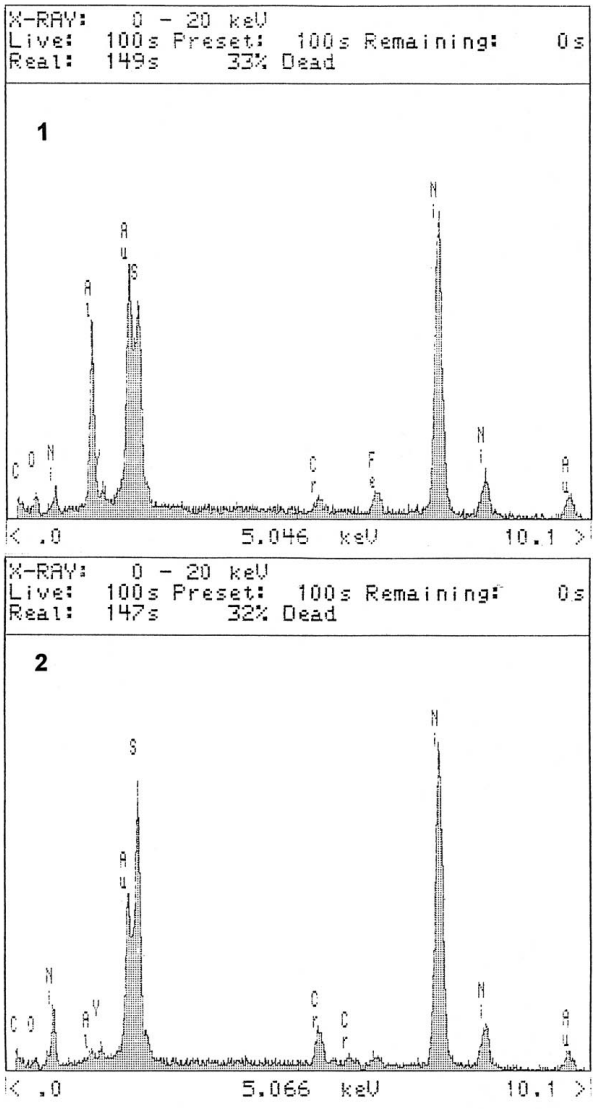

(b)

Figure 3 a) SEM image and b) EDX analysis of the surface of the material Ni22Cr10Al1Y of lower porosity and smaller grains exposed in H_2/H_2S mixture at $p_{S_2} = 1$ Pa and 1273 K (Au peaks result from the surface deposition of gold before SEM/EDX analysis).

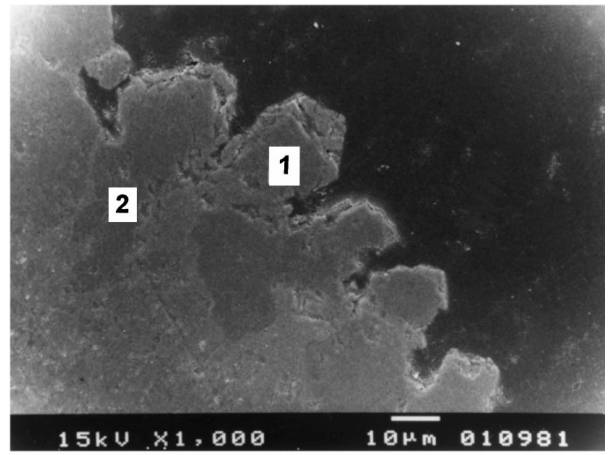

(a)

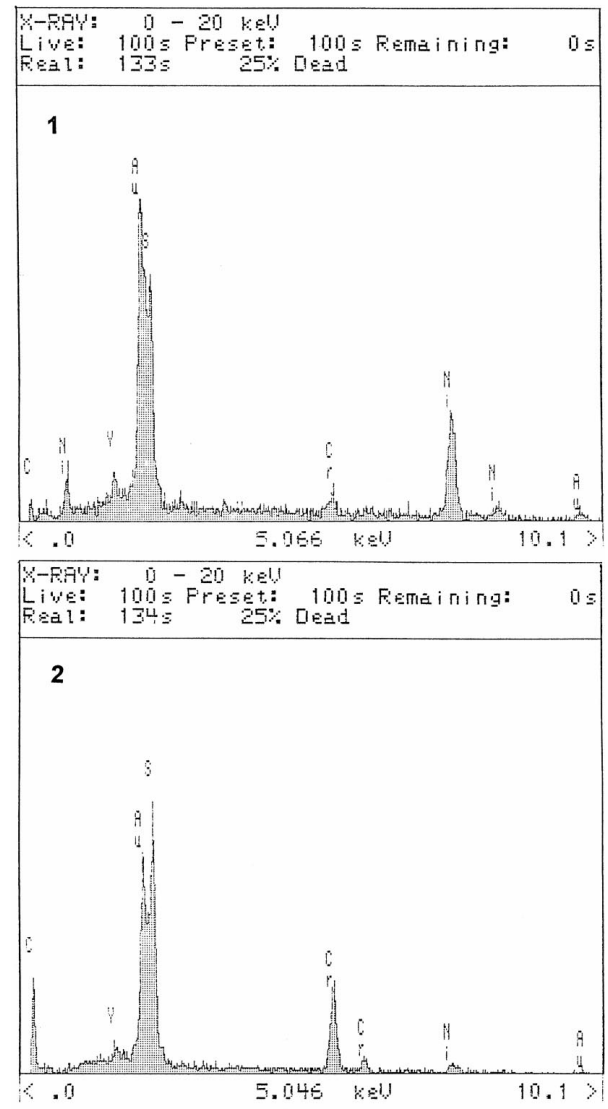

(b)

Figure 4 a) SEM image and b) EDX analysis of the polished cross-section of the material Ni22Cr10Al1Y of lower porosity and smaller grains exposed in H_2/H_2S atmosphere at $p_{S_2} = 1$ Pa and 1273 K (Au peaks result from the surface deposition of gold before SEM/EDX analysis).

of low porosity and small grains exposed at $p_{S_2} = 1$ Pa and 1273 K are presented, as an example, in Figs 3–4. It follows from these analysis that for $p_{S_2} = 1$ Pa, an external Ni_3S_2 layer was formed. From XRD data obtained from the powdered scale (Table I) it follows than that beneath this external layer a mixture of the sulphides Cr_2S_3, Al_2S_3 and sulphospinel $NiCr_2S_4$ was formed. The sulphidation products formed on both materials

were practically identical regarding their phase composition. Only small quantitative differences were observed. The nickel sulphide formed a thin outermost layer from which the burls grew up in the form of big blisters and cylinders. The type of those burls indicates that they were the solidified dripstones of Ni_3S_2/Ni eutectics which subsequently reacted further forming the nickel sulphide. None of the other alloy components was detected in burls.

The SEM image and EDX analysis of the surface of the material of low porosity and small grains exposed at $p_{S_2} = 10^{-3}$ Pa and 1273 K are presented, as an example, in Fig. 5. From this analysis it follows that for $p_{S_2} = 10^{-3}$ Pa a thin external layer of the Cr_2S_3 and Cr_7S_8 chromium sulphides was formed. From XRD data obtained from the powdered scale (Table I) it follows that beneath this layer, the chromium sulphide and aluminium sulphide were formed.

The nickel sulphide because of the thermodynamic restrictions, could embody only the sulphospinel structure of $(Cr,Ni)Al_2S_4$ formula.

Fractured cross-section and EDX analysis of the alloy of smaller grains exposed in SO_2 at 1273 K is presented in Fig. 6. Practically the same image is for the material having coarser grains. A thin layer comprising a mixture of the simple and complex oxides of alloy components NiO, Al_2O_3, Cr_2O_3, $NiCr_2O_4$ was formed on the surface of these materials. None of the detected oxides formed any separate, continuous and compact layer or sub-layer. The greenish colour of the specimens surfaces indicated that the main components of the formed scale was the chromium oxide. In some regions on the surface of the scale a higher aluminium concentration was detected. Inside the scale, the trace amounts of the chromium sulphide and of the sulphospinel of formula $NiCr_2S_4$ as well as of the garnet-type compound $Y_3Al_5O_{12}$ (YAG) [9] were found.

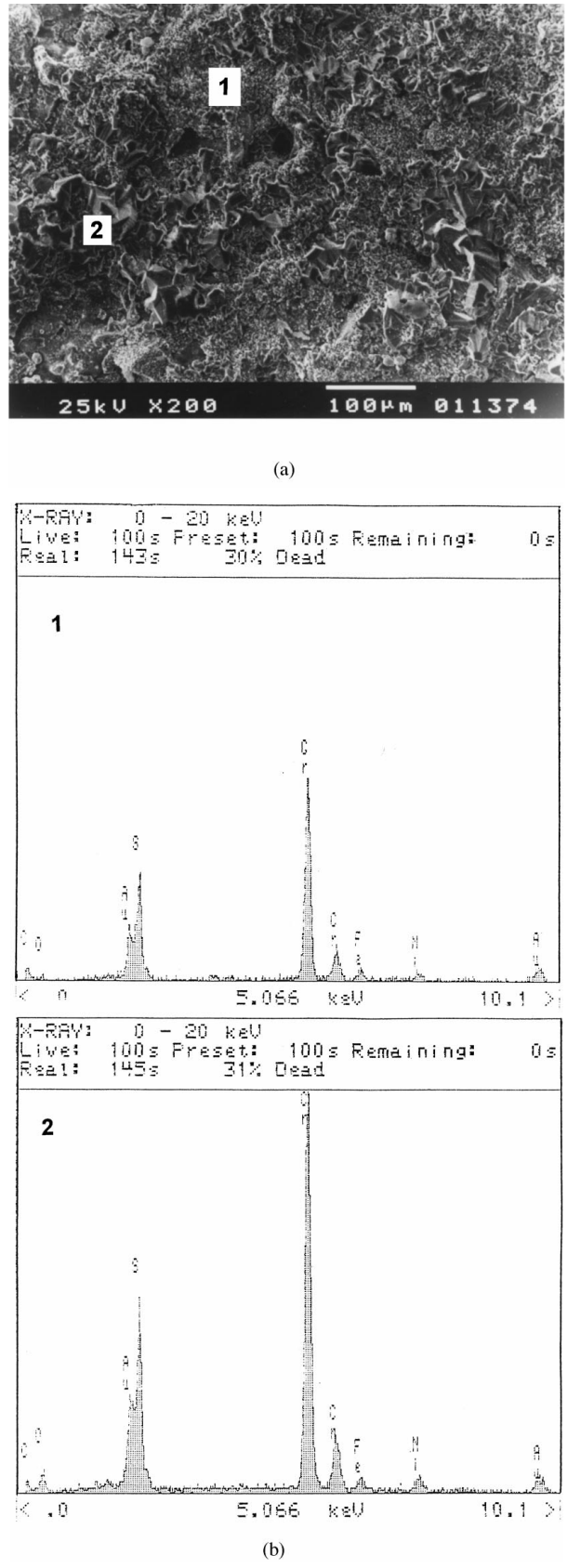

Figure 5 a) SEM image and b) EDX analysis of the surface of the material Ni22Cr10Al1Y of lower porosity and smaller grains exposed in H_2/H_2S atmosphere at $p_{S_2} = 10^{-3}$ Pa and 1273 K (Au peaks result from the surface deposition of gold before SEM/EDX analysis).

4. Discussion

The sulphidation rate of the material of lower porosity and smaller grains was found to be slightly higher than that of the material with higher porosity and coarser grains at all the applied sulphidation conditions. It increased with increasing reaction temperature, what indicates that the sulphidation process was controlled by diffusion of the reactants through the scale. The sulphidation reaction rate for both materials increased with increasing sulphur vapour pressure. This resulted from the completely different structure of the scale since, as it has been already mentioned, at low sulphur vapour pressure ($p_{S_2} = 10^{-3}$ Pa) the possibility of the formation of the nickel sulphide on the Ni22Cr10AlY alloy is to be excluded. The sulphidation rates of both materials are comparable to those found for Ni23Co19Cr12Al alloys sulphidised at the same conditions [4, 10].

In Table II the parabolic sulphidation rate constants k_p, calculated for both investidated materials are compared with the corresponding literature data concerning oxidation of other alloys. The rate constants obtained in this work are about two-three orders of magnitude greater than those from the literature. This difference results from much higher porosity of sprayed materials than vacuum inductcion melted alloys.

In Table III the parabolic oxidation rate constants k_p in SO_2 obtained for both materials at 1173 and 1273 K

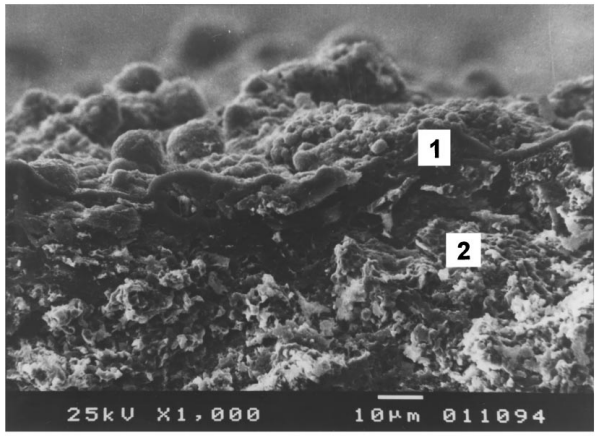

(a)

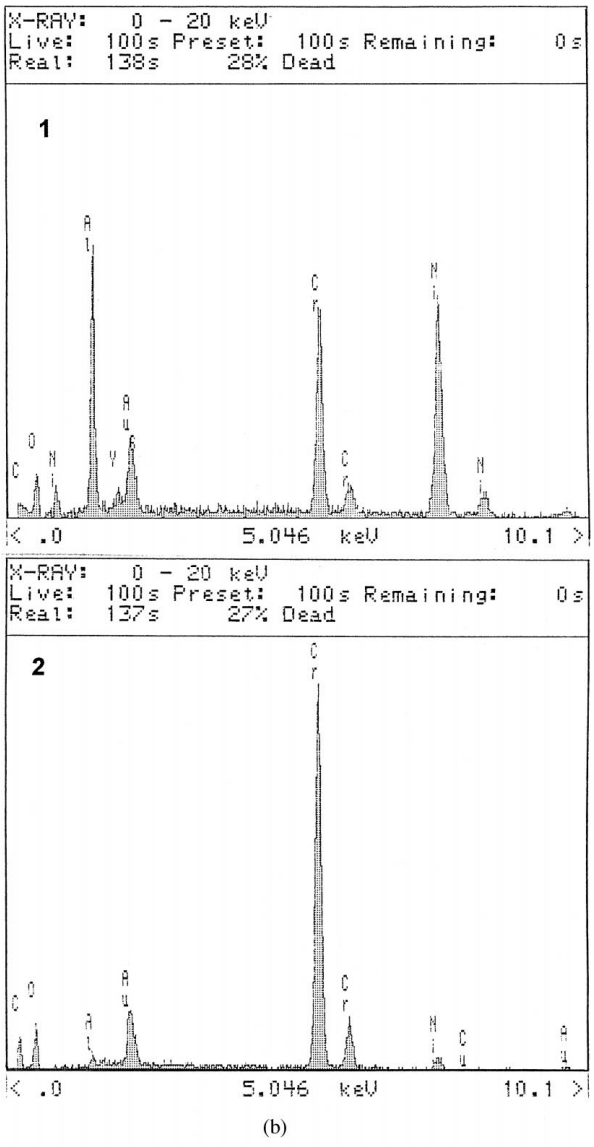

(b)

Figure 6 a) SEM image and b) EDX analysis of the fractured cross-section of the material Ni22Cr10Al1Y of lower porosity and smaller grains exposed in SO_2 atmosphere at 1273 K (Au peaks result from the surface deposition of gold before SEM/EDX analysis).

are compared with the corresponding literature data for chromia and alumina formers oxidized in air and oxygen. It appears that the k_p-values for the alloy having lower porosity and smaller grains are two or more orders of magnitude higher than those for chromia and/or alumina forming materials. The k_p-values for the alloy having higher porosity and coarser grains are comparable with those of a few reactive elements-free alloys (positions 5, 6 and 16 in Table III). They are considerably higher than the parabolic rate constants of yttrium-bearing alloys.

From XRD and SEM/EDX analysis and thermodynamic considerations it follows that under the nickel sulphide layer a porous layer consisting of the Cr_2S_3 and Al_2S_3 mixture and of the $NiCr_2S_4$ spinel was formed for the materials exposed at $p_{S_2} = 1$ Pa. The lack of any distinct sulphidation layers resulted from the porous structure of the initial material, which enabled enhanced migration of the sulphur particles towards the interior of the material and formation of the nickel sulphide. Thus, the initially developed nickel sulphide subsequently formed the eutectics with the nickel and floated outwards forming the mentioned above burls.

Inside the specimen various discontinuities (pores, cavities and fissures) were left as a result of the flow-out of the liquid Ni_3S_2/Ni phase. This explanation may be supported by the fact that no other reaction front boundary was detected. It was found, however, that on the outer surface of the nickel sulphide the elemental yttrium appeared which might be due to its previous doping of the nickel sulphide scale.

The observed microstructures are consistent with the observed sulphidation kinetics. The sulphidation rate of both alloys at the sulphur vapour pressure $p_{S_2} = 1$ Pa was by two orders of magnitude higher than that at $p_{S_2} = 10^{-3}$ Pa. The thermodynamically stable nickel sulphide, formed at the sulphur vapour pressure $p_{S_2} = 1$ Pa, exhibits significantly higher defect concentration within the cation sublattice than the chromium sulphide which is the main component of the scale formed on the alloys sulphidised at the lower sulphur vapour pressure (10^{-3} Pa). The higher amount of defects enhances the transport of cations, being nickel ions, through the scale as well as the possibility of doping of trivalent yttrium ions in cation sublattice which increases the concentration of defects.

Yttrium was usually detected at the surface of grains in the outermost part of scale. Smell of the H_2S in the reaction tube after the experiment pointed out that probably Al_2S_3 or another compound could form in the scale. Analysis of the fractured and polished cross-sections of the specimens after exposure indicated that the sulphidation process of the studied alloys proceeded preferentially along the discontinuities and grain boundaries, where sulphur rich areas were detected.

From the equilibrium phase diagram of Ni-O-S system [3] it follows that only NiO and/or $NiSO_4$ are stable phases in SO_2 under studied conditions. Therefore, the mechanism of the sulphide formation in the SO_2 atmosphere needs explanation. Because of lack of direct method of studying this mechanism, and because of complexity of the oxidation process any explanation has to be somewhat speculative. The applied SO_2 almost always contains some impurities of oxygen. At the equilibrium conditions, in the $SO_2 + O_2$ mixture with a relatively high content of the oxygen impurity

TABLE II Comparison of parabolic rate constants k_p obtained in this work (sulphidation of Ni22Cr10Al1Y in H_2/H_2S) with the literature data of the sulphidation of Ni, Fe, Cr, Al alloys

No.	Alloy	Oxidation conditions		k_p ($g^2\ cm^{-4}\ s^{-1}$) (parabolic)	Ref.
		T (K)	p_{S_2} (Pa)		
This study:					
1	Ni22Cr10Al1Y—larger grains, higher porosity	1273	1×10^{-3}	1.4×10^{-9}	
2	Ni22Cr10Al1Y—larger grains, higher porosity	1273	1	5.8×10^{-7}	
3	Ni22Cr10Al1Y—smaller grains, lower porosity	1273	1×10^{-3}	5.3×10^{-9}	
Ni based alloys:					
4	Ni48A14Cr (vacuum induction melting)	1173	0.32	3×10^{-9}	[11]
5	Ni48Al4Cr (vacuum induction melting)	1273	0.32	7×10^{-8}	[11]
6	Ni48Al4Cr (vacuum induction melting)	1173	1×10^{-3}	1×10^{-11}	[11]
7	Ni48Al4Cr (vacuum induction melting)	1273	1×10^{-3}	2×10^{-12}	[11]
8	Ni51.8Al (vacuum induction melting)	1173	1	1×10^{-10}	[12]
Fe based alloys:					
9	Fe26Cr (vacuum induction melting)	1073	1×10^{-3}	1×10^{-8}	[13]
10	Fe23.4Cr18.6Al	1073	1×10^{-3}	1×10^{-10}	[9]
11	Fe26.6Cr	1073	1×10^{-3}	1×10^{-7}	[9]

TABLE III Comparison of parabolic rate constants k_p obtained in this work (oxidation of Ni22Cr10Al1Y in SO_2) with the literature data of the oxidation of Ni, Cr, Al, Y alloys in air and oxygen

No.	Alloy	Oxidation conditions		k_p ($g^2\ cm^{-4}\ s^{-1}$) (parabolic)	Ref.
		T (K)	Gas		
This study:					
1	Ni22Cr10Al1Y—larger grains, higher porosity	1173	SO_2	2.1×10^{-11}	
2	Ni22Cr10Al1Y—larger grains, higher porosity	1273	SO_2	5.8×10^{-11}	
3	Ni22Cr10Al1Y—smaller grains, lower porosity	1173	SO_2	8.3×10^{-11}	
4	Ni22Cr10Al1Y—smaller grains, lower porosity	1273	SO_2	9.9×10^{-9}	
Chromia formers:					
5	Ni30Cr	1273	O_2, 10^4 Pa	2×10^{-11}	[14]
6	Ni40Cr	1273	O_2, 10^5 Pa	5×10^{-11}	[15]
7	Ni20Cr-3 vol.% Y_2O_3	1273	O_2, 1.3×10^4 Pa	6×10^{-13}	[16]
8	Ni20Cr-3 vol.% Y_2O_3	1273	Air	3×10^{-13}	[17]
Alumina formers:					
9	Ni13Al	1273	Air	5×10^{-13}	[18]
10	Ni10Cr5Al	1273	Air	6×10^{-13}	[19]
11	Ni10Cr5A10.5Y	1273	Air	4×10^{-13}	[19]
12	Ni16Cr6A10.1Y	1273	Air	5×10^{-14}	[20]
13	Ni16Cr6A10.3Y	1356	O_2, 10^5 Pa	2×10^{-12}	[21]
14	Ni18Cr12Al0.3Y	1356	O_2, 10^5 Pa	6×10^{-12}	[21]
15	Ni35Cr6A10.95Y	1356	O_2, 10^5 Pa	6×10^{-12}	[21]
16	Ni20.7Cr8.8Al	1373	Air	7×10^{-11}	[22]
17	Ni20.7Cr8.8Al1.0Y	1373	Air	2×10^{-12}	[23]

in the sulphur dioxide reaching up to about 0.01%, the sulphur partial pressure falls drastically a few orders of magnitude lower than the dissociation pressures of nickel and chromium sulphides. The SO_2 gas, when migrating through pores and other discontinuities into the inner part of the material reacts with it forming the oxides of the alloy components. This consumption of the oxygen leads to some increase of the sulphur partial pressure. As the latter becomes higher than the dissociation pressure of either chromium or nickel sulphide, these compounds might be formed. This hypothesis seems to be supported by the fact that the areas with the presence of the sulphur have been detected always in the pores and discontinuities of the studied material.

Because the porosity of studied materials may considerably affect the oxidation process, it is difficult to elucidate their degradation mechanisms more in detail. This problem even raises its validity when these materials are applied in the form of thin layer bond coats. The local effects are expected to play an important role in the degradation process which, thus, should be studied using more adequate and sometimes dedicated methods enabling direct analysis of the gas in the reaction zone and getting information from small regions.

5. Conclusions

From this study of the corrosion behaviour of Ni22Cr10AlY alloy in sulphur-containing atmospheres the following conclusions can be drawn:

1. At high sulphur vapour pressures, $p_{S_2} = 1$ Pa, the destruction of the alloys studied here proceeds instantly due to the formation of highly defective and fast-growing nickel sulphide Ni_3S_4.

2. At low sulphur vapour pressures, $p_{S_2} = 10^{-3}$ Pa, the rate of sulphidation considerably decreases due to the formation of more protective layers of chromium sulphides and sulphospinels $(Cr,Ni)Al_2S_2$.

3. Yttrium appears only on the surface of nickel sulphide presumably as a built-in trivalent cation dopant into the nickel sulphide lattice.

4. The rate of sulphidation of the alloy having smaller grains and lower porosity is higher than that of the material exhibiting coarser grains and higher porosity which means that the material of higher porosity with larger grains suffers the sulphidation treatment more slowly than that of a lower porosity with smaller grains.

5. The oxidation process in SO_2 atmosphere follows the parabolic law at both used temperatures (1173 and 1273 K); the material of smaller grains and lower porosity oxidises faster than the material of larger grains and higher porosity.

6. On the surface of the studied materials exposed in SO_2 a thin scale layer is a mixture of the nickel, aluminium and chromium oxides and of chromium-nickel spinel.

7. In the oxide scale formed in SO_2, trace amounts of the aluminium sulphide appear only in some areas in the scale.

Acknowledgements

This work has been carried out under contracts No CIPA-CT94-0119 supported by EC COPERNICUS.

References

1. F. J. PENNESI and D. K. GUPTA, *Thin Solid Films* **84** (1981) 49.
2. S. J. SHAFFER, D. H. BOONE, R. T. LAMBERTSON and D. PEACOCK, *ibid.* **107** (1983) 463.
3. M. FRANCES, M. VILASI, M. MANSOUR-GABR, J. STEINMETZ and P. STEINMETZ, *Mat. Sci. Eng.* **88** (1987) 89.
4. E. GODLEWSKA, E. ROSZCZYNIALSKA and Z. ŻUREK, *High Temp. Mat. Proces.* **13** (1994) 259.
5. J. GAWEL and A. WYCZESANY, *Corr. Sci.* **28** (1988) 867.
6. S. MROWEC and T. WERBER, in "Korozja Gazowa Metali" (Wydawnictwo "Śląsk", 1975) p. 425.
7. J. GILEWICZ-WOLTER, *Zeszyty Naukowe AGH* **22** (1990) 56.
8. Z. ŻUREK, *J. Thermal Anal.* **39** (1993) 15.
9. T. NARITA and T. ISHIKAWA, *Mater. Sci. Eng.* **A120** (1989) 31.
10. E. GODLEWSKA, E. ROSZCZYNIALSKA and Z. ŻUREK, *Werkstoffe u. Korrosion* **45** (1994) 341.
11. E. GODLEWSKA, E. ROSZCZYNIALSKA, A. RAKOWSKA, S. MROWEC and Z. ŻUREK, *Solid State Phen.* **41** (1995) 205.
12. K. GODLEWSKI, E. GODLEWSKA, S. MROWEC and M. DANIELEWSKI, *Mater. Sci. Eng.* **A120** (1989) 31.
13. Z. ŻUREK and J. GAWEL, *J. Phys. IV, Coll. 9, suppl. au J. Phys. III* **3** (1993) 327.
14. C. S. GIGGINS and F. S. PETTIT, *Trans. Metall. Soc. AIME* **245** (1969) 2495.
15. T. HODGKIESS, G. C. WOOD, D. P. WHITTLE and B. D. BASTOW, *Oxid. Met.* **14** (1980) 85.
16. J. STRINGER, B. A. WILCOX and R. I. JAFFEE, *ibid.* **5** (1972) 11.
17. H. T. MICHELS, *Met. Trans.* **7A** (1976) 379.
18. J. D. KUENZLY and D. L. DOUGLASS, *Oxid. Met.* **8** (1974) 139.
19. A. KUMAR, M. NASRALLAH and D. L. DOUGLASS, *ibid.* **8** (1974) 227.
20. C. S. GIGGINS and F. S. PETTIT, in Report ARL 75-0234 (Pratt and Whitney Aircraft, Connecticut, 1975).
21. W. J. BRINDLEY and R. A. MILLER, *Surf. Coat. Technol.* **43/44** (1990) 446.
22. P. CHOQUET, C. INDRIGO and R. MEVREL, *Mat. Sci. Eng.* **88** (1987) 97.
23. M. TAWANCY, N. M. ABBAS and A. BENNETT, *Surf. Coat. Technol.* **68/69** (1994) 10.
24. J. MUSIL and P. FIALA, *Surf. Coat. Technol.* **52** (1992) 211.
25. S. MROWEC and T. WERBER, in "Korozja Gazowa Metali" (Wydawnictwo "Śląsk", 1975) p. 448.

Received 19 June 1998
and accepted 22 July 1999